

Article

Genome-Wide Identification and Analysis of MYB Transcription Factors in *Pyropia yezoensis*

Xinzi Yu ¹, Lei Tang ¹, Xianghai Tang ¹ and Yunxiang Mao ^{2,3,*} 

¹ MOE Key Laboratory of Marine Genetics and Breeding, College of Marine Life Sciences, Ocean University of China, Qingdao 266003, China

² MOE Key Laboratory of Utilization and Conservation of Tropical Marine Bioresource & Yazhou Bay Innovation Institute, Hainan Tropical Ocean University, Sanya 572022, China

³ Laboratory for Marine Biology and Biotechnology, Qingdao National Laboratory for Marine Science and Technology, Qingdao 266237, China

* Correspondence: yxmao@hntou.edu.cn

Abstract: MYB transcription factors are one of the largest transcription factor families in plants, and they regulate numerous biological processes. Red algae are an important taxonomic group and have important roles in economics and research. However, no comprehensive analysis of the MYB gene family in any red algae, including *Pyropia yezoensis*, has been conducted. To identify the MYB gene members of *Py. yezoensis*, and to investigate their family structural features and expression profile characteristics, a study was conducted. In this study, 3 R2R3-MYBs and 13 MYB-related members were identified in *Py. yezoensis*. Phylogenetic analysis indicated that most red algae MYB genes could be clustered with green plants or Glaucophyta MYB genes, inferring their ancient origins. Synteny analysis indicated that 13 and 5 *PyMYB* genes were orthologous to *Pyropia haitanensis* and *Porphyra umbilicalis*, respectively. Most Bangiaceae MYB genes contain several Gly-rich motifs, which may be the result of an adaptation to carbon limitations and maintenance of important regulatory functions. An expression profile analysis showed that *PyMYB* genes exhibited diverse expression profiles. However, the expression patterns of different members appeared to be diverse, and *PyMYB5* was upregulated in response to dehydration, low temperature, and *Pythium porphyrae* infection. This is the first comprehensive study of the MYB gene family in *Py. yezoensis* and it provides vital insights into the functional divergence of MYB genes.

Keywords: transcription factors; MYB superfamily; red algae; *Pyropia yezoensis*; phylogenetic analysis; gene function



Citation: Yu, X.; Tang, L.; Tang, X.; Mao, Y. Genome-Wide Identification and Analysis of MYB Transcription Factors in *Pyropia yezoensis*. *Plants* **2023**, *12*, 3613. <https://doi.org/10.3390/plants12203613>

Academic Editor: Nobutoshi Yamaguchi

Received: 9 September 2023

Revised: 6 October 2023

Accepted: 11 October 2023

Published: 19 October 2023



Copyright: © 2023 by the authors. Licensee MDPI, Basel, Switzerland. This article is an open access article distributed under the terms and conditions of the Creative Commons Attribution (CC BY) license (<https://creativecommons.org/licenses/by/4.0/>).

1. Introduction

As one of the three ancient plant groups, red algae originated from a primary photosynthetic endosymbiosis event and donate plastids that form numerous other photosynthetic lineages. Thus, red algae have contributed dramatically to broader eukaryotic evolution and diversity [1]. Some red algae also have important economic value and create important economic results. *Pyropia yezoensis* (nori) belongs to Bangiales (Rhodophyta), which is the most genetically diverse order of red algae and is a principal species used in the economic cultivation of edible seaweed [2].

Transcription factors (TFs), such as MYB, WRKY, and bZIP, play essential roles in plant molecular stress regulation [3]. Among the various TF families in the genome, the MYB family is one of the largest and most functionally diverse families [4]. Thus, it is usually called the MYB superfamily. MYB superfamily proteins are characterized by a highly conserved MYB domain at their N-terminus, which is usually composed of 1–4 adjacent imperfect tandem repeats. MYB proteins can be divided into different classes depending on the number of MYB imperfect tandem repeats (Rs): 4R-MYB proteins (having four Rs),

R1R2R3-MYB proteins (*3R-MYB*, having three Rs), *R2R3-MYB* proteins (having two Rs), and *MYB*-related proteins (*1R-MYB*, having one R) [5].

The first plant *MYB* gene, C1, was isolated in maize in the 1980s [6]. Since then, different aspects of the *MYB* gene family, such as gene number, sequence characterization, evolution, and functions, have been broadly studied in plants [7–16]. Among the four classes, *4R-MYB* is the smallest. Each gene in this class contains four R1/R2 repeats, but little is known about these proteins in plants [4]. The *3R-MYB* proteins have been found in most eukaryotic genomes, and these proteins play a role in controlling the progression of mitosis and cytokinesis [17]. Among these four classes, *R2R3-MYB* is the largest in higher plants and is thought to have evolved from the *R1R2R3-MYB* gene ancestors by losing the sequences encoding R1 repeats [18]. However, it has also been proposed that *3R-MYB* genes are derived from *R2R3-MYB* genes by obtaining sequences encoding the R1 repeat through ancient intragenic duplication [19]. Higher plants have numerous *R2R3-MYB* genes, which are in accordance with their multiple roles in life processes [20]. The *R2R3-MYB* gene family is widely involved in the regulation of various biological processes, including secondary metabolism [21,22], cell fate and identity [23,24], and organ development [25–27]; in addition, most *R2R3-MYB* genes have been suggested to regulate plant responses to biotic and abiotic stress conditions [28–34]. The fourth class of the *MYB* family contains a single or partial *MYB* repeat and is mainly involved in the control of cellular morphogenesis, secondary metabolism, and circadian rhythm [35,36]. Overall, *MYBs* have diverse functions and play an important role in plant stress tolerance, plant growth, and development.

Extensive studies on various plant species have improved our understanding of the *MYB* gene family in different species [7–16]. However, a genome-wide analysis of the *MYB* gene family is mainly from studies in green-lineage plants, and little is known about red algae. Currently, only three *R2R3-MYB* genes and five *MYB*-related genes have been identified in *Cyanidioschyzon merolae* [30,37], three *R2R3-MYB* genes in *Chondrus crispus*, three *R2R3-MYB* genes in *Galdieria sulphuraria*, and three *R2R3-MYB* genes in *Porphyra umbilicalis* [30]. Moreover, in these studies, red algae *MYB* genes have been used as an outgroup of research related to green plants and have never been the protagonist of research. In short, systematic and comprehensive studies on the *MYB* gene family in algae are lacking.

Pyropia yezoensis has interesting biological characteristics that have attracted the attention of researchers [38]. For example, *Py. yezoensis* has a complex life cycle alternating between two independent complex multicellular stages that are morphologically distinct: the gametophyte (haploid) and the sporophyte (diploid). The alternating heteromorphic generations might have evolved to respond to different inorganic carbon availability [39]. The edible, leafy thallus (gametophyte) inhabits the upper intertidal zone of exposed coasts, suffering fluctuating environmental stress, such as extreme drought and high temperature [38,39]. For this reason, the *Py. yezoensis* thallus, which is capable of tolerating broad and extreme environmental stress, is of interest as a model for studying the molecular mechanisms of stress resistance. The high-quality chromosomal genome of *Py. yezoensis* and available transcriptomic data also provide convenient resources and lay the foundation for the complete identification of *MYB* genes in *Py. yezoensis* [39–42].

MYBs are the key to regulatory networks controlling development and responses to abiotic and biotic stress, and *Py. yezoensis* has unique physiological and growth characteristics. This study was conducted to identify the *MYB* gene members of *Py. yezoensis* (*PyMYBs*) and to fully investigate their family features and expression profile characteristics. In this study, all non-redundant members of the *MYB* genes in *Py. yezoensis* were screened from available, high-quality, chromosomal-level genomes. We determined the characteristics of *PyMYB* genes based on their physicochemical properties, genomic locations, conserved motifs, and promoters. Then, we analyzed the phylogenetic relationships of these genes combined with *MYBs* in seven other red algae species, three green algae species, and one Glaucophyta species. In addition, the expression levels of the nori *MYB* genes in two life cycle stages and different blade parts, as well as in response to dehydration, temperature, and

disease infection stress, were analyzed. Our findings will provide useful resources for future research on the functions of algae MYB genes and help us understand the evolutionary history of MYB genes in different species.

2. Results

2.1. Genome-Wide Identification of PyMYB Genes in *Py. yezoensis*

A total of 41 candidate sequences containing MYB or MYB-like domains were identified in *Py. yezoensis*. Twenty-five *PyMYB* candidates were discarded because they lacked a complete MYB domain or complete gene structure in the confirmatory step. The putative novel MYB sequences yielded a dataset of 16 nonredundant MYB genes containing 3 R2R3-MYB proteins and 13 MYB-related proteins (Table 1). All 16 MYB sequences were designated as *PyMYB1–3* (R2R3-MYB) or *PyMYB4–16* (MYB-related genes), according to their classification and genomic distribution in *Py. yezoensis*. Table 1 lists the gene ID, chromosomal location, gene length (ranging from 1394 to 6446 bp), number of introns (ranging from 0 to 2), number of amino acids (ranging from 263 to 1693 amino acids), isoelectric point (pI, ranging from 5.25 to 11.05), molecular weight (MW, ranging from 25.75 to 169.47 kDa), and instability index (ranging from 42.03 to 71.18). Among the 16 *PyMYB* genes, most lacked introns, accounting for half of the *PyMYB* genes, followed by the *PyMYB* genes with one intron and two introns (six and two, respectively) (Table 1, Figure 1A). On the basis of the starting positions of the MYB genes within the chromosomes, the 16 *PyMYB* genes were unevenly distributed among the three nori chromosomes (Figure 1B). The number of *PyMYB* genes on chromosomes 1, 2, and 3 was five, seven, and four, respectively; among them, R2R3-MYB was only present on chromosomes 2 and 3 (Table 1). With the same strategy, a total of 171 MYB-related genes, 78 R2R3-MYBs, 9 3R-MYBs, and 3 4R-MYBs, were also identified from the other seven red algae species (*Porphyra umbilicalis*, *Chondrus crispus*, *Cyanidioschyzon merolae*, *Gracilariopsis chorda*, *Porphyridium purpureum*, and *Galdieria sulphuraria*), three green algae species (*Chlamydomonas reinhardtii*, *Micromonas pusilla*, and *Chara braunii*), and one Glaucophyta species (*Cyanophora paradoxa*) (Tables S2 and S3).

Table 1. Characteristics of *PyMYB* genes.

No.	Gene ID	Chr.	Location Coordinates (5'–3')	Gene Length (bp)	Introns	Protein			Instability Index
						Length (aa)	pI	MW (Da)	
<i>PyMYB1</i>	py05834	Chr_2	20,775,567–20,777,675(–)	2109	0	655	9.65	65,595.95	71.18
<i>PyMYB2</i>	py09814	Chr_2	29,201,221–29,204,172(–)	2952	0	954	9.71	92,734.27	56.15
<i>PyMYB3</i>	py09955	Chr_3	1,412,341–1,414,602(–)	2262	1	663	8.4	65,431.41	46.32
<i>PyMYB4</i>	py08181	Chr_1	9,248,952–9,251,564(+)	2613	1	870	6.14	85,547.49	45.30
<i>PyMYB5</i>	py00388	Chr_1	15,749,165–15,752,214(–)	3050	1	636	8.17	69,882.18	43.76
<i>PyMYB6</i>	py10564	Chr_1	19,596,875–19,602,348(+)	5474	0	1693	5.25	169,473.82	54.09
<i>PyMYB7</i>	py03838	Chr_1	30,760,790–30,762,242(–)	1453	0	465	10.37	45,669.49	49.07
<i>PyMYB8</i>	py08093	Chr_1	42,710,239–42,712,056(–)	1818	0	562	7.63	59,193.78	44.60
<i>PyMYB9</i>	py08650	Chr_2	2,996,682–3,001,254(–)	4573	1	1283	10.17	126,648.01	64.16
<i>PyMYB10</i>	py09282	Chr_2	12,729,693–12,731,086(+)	1394	2	263	9.56	25,747.1	53.78
<i>PyMYB11</i>	py06564	Chr_2	24,928,598–24,935,043(+)	6446	1	900	8.84	93,136.05	42.03
<i>PyMYB12</i>	py07923	Chr_2	31,305,719–31,310,122(+)	4404	0	1425	11.05	143,276.79	55.83

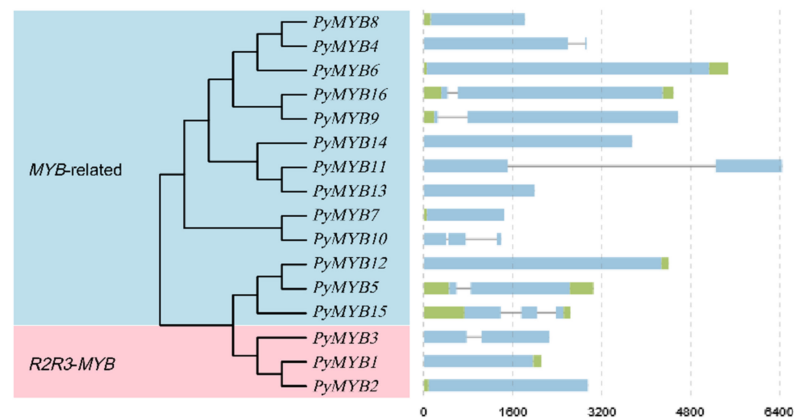
Table 1. Cont.

No.	Gene ID	Chr.	Location Coordinates (5'–3')	Gene Length (bp)	Introns	Protein			Instability Index
						Length (aa)	pI	MW (Da)	
<i>PyMYB13</i>	py08311	Chr_2	31,620,311–31,622,302(–)	1992	0	663	10.39	65,237.37	69.35
<i>PyMYB14</i>	py05796	Chr_3	726,004–729,747(–)	3744	0	1247	6.67	111,473.37	54.42
<i>PyMYB15</i>	py01811	Chr_3	13,184,111–13,186,746(–)	2636	2	360	8.59	33,652.99	68.39
<i>PyMYB16</i>	py04398	Chr_3	24,701,888–24,706,378(–)	4491	1	1268	10.28	125,218.85	65.42

A

Gene Structure

■ CDS
■ UTR



B

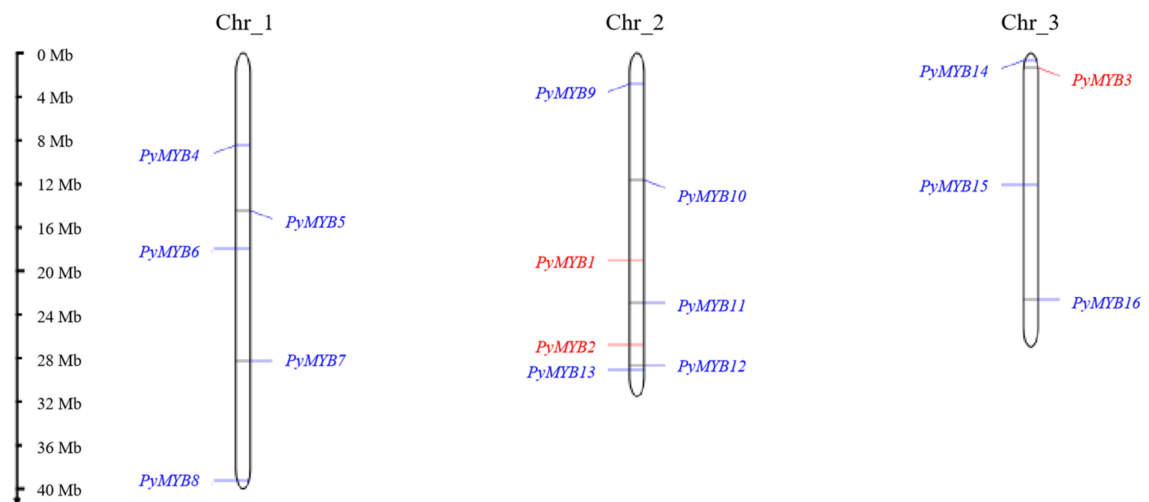


Figure 1. (A) Phylogenetic tree and gene structures of *PyMYB* genes. (B) Chromosomal location of *PyMYB* genes. Red color, R2R3-MYB genes; blue color, MYB-related genes.

2.2. Phylogenetic Analysis of *PyMYB* Genes

Because the sequences of R2R3-MYB and MYB-related proteins outside the MYB-binding domains were highly diverse, only the MYB-binding domains (Rs) were used to reconstruct phylogenetic trees.

First, the ML tree was built on the basis of 206 R2R3-MYB protein sequences from 13 representative species of different taxonomic groups, including eight red algae species, three green algae species, one Glaucophyta species, and *Arabidopsis thaliana* (Figures S1 and S2,

Tables S2 and S4). The *R2R3-MYB* genes were then divided into 13 subgroups with robust bootstrap (generally $\geq 60\%$): G1–G13 (Figures S1 and S2). Overall, the *MYB* genes of eight red algae species were located in most basal clades in the phylogenetic tree, suggesting their ancient origin. Red algae *R2R3-MYB* genes were classified as G2, G3, G4, G5, G7, G9, G10, G11, G12, and G13. Except for genes in G2, G3, and G7, other *R2R3-MYB* genes of red algae were grouped with genes of green plants or glaucophytes. The *R2R3-PyMYBs* belonged to the G4, G5, and G12 subgroups.

An ML tree was also built on the basis of 247 *MYB*-related protein sequences from 13 representative species from different taxa (Figures S3 and S4, Tables S2 and S4). These *MYB*-related genes were divided into subgroups with robust bootstraps (generally $\geq 60\%$): CCA1-like/R-R-type, TBP-like, I-box-like, TRF-like, and CPC-like subgroups, which have been well-grouped in previous studies [37,43] and seven new groups (NG1–NG7) (Figures S3 and S4). The I-box-like and TRF-like subgroups did not contain any red algae *MYB*-related genes, which is consistent with a previous study [37]. In addition, the CCA1-like/R-R-type, TBP-like, CPC-like, NG1, NG2, NG4, NG5, and NG6 subgroups contained red algae *MYB*-related genes and genes from other Archaeplastida lineages, particularly genes from glaucophytes, suggesting their ancient origin; the *MYB*-related *PYMYBs* were scattered in almost all these subgroups except for NG6 and NG7.

Inevitably, through a comparative analysis of two types of ML trees, the topological structure was not very fixed in some genes, including GsuXP005704452, GsuXP_005703373, CcXP_005713040, and CcXP_005717760; in this study, they were finally grouped by subsequent motif composition analysis. In the future, the classification will be improved with the continuous enrichment of red algae genomes and the addition of more red algae *MYB* genes for analysis.

2.3. Motif Structure and Synteny Analysis

The similarities in motif organization among genes can be used as evidence to support their common origins. Ten conserved motifs were identified in the *MYB* proteins using MEME software (<https://meme-suite.org/meme/> accessed on 10 October 2023) (Figures 2 and 3, Table 2). Motifs 1 and 4 encoded the *MYB* DNA-binding domain, and the number of these two motifs in the *MYB* genes of red algae was consistent with their classification in the identification pipeline. In general, *MYB* genes in the same subgroup shared a similar motif composition, and this phenomenon was more obvious in the adjacent genes of the species that were closely related, such as *PyMYB2* and *Ph05827/PuOSX69724*, *PyMYB3* and *Ph04980*, *PyMYB4* and *Ph09887*, *PyMYB5* and *Ph02171/PuOSX76044*, *PyMYB6* and *Ph02359*, *PyMYB7* and *Ph08492*, *PyMYB8* and *Ph06857/PuOSX75147*, *PyMYB9* and *Ph07942*, *PyMYB12* and *Ph05957*, *PyMYB14* and *Ph05025*, and *PyMYB16* and *Ph09161*. The similarity in their motif composition may imply that they originated from the same duplication event and that these genes' functions might be conservative and important. However, these gene pairs with similar motif compositions had different gene structures, indicating that each species also experienced species-specific evolutionary events.

Table 2. Motif information of *MYB* proteins in eight red algae.

Motifs	Width (aa)	Pfam ($p < 1 \times 10^{-5}$)	Sequences
Motif1	43	Myb DNA-binding domain	SIKRGWWTEEEDELLELLKLGGRNWKRIAKHLPGRDTNQCERS
Motif2	69	SWIRM domain	LPEFFLGRFASKTPEVYKQYRBFMIDTWRQDPTRYLTATAVR RHLAGDACAILRVHAFLEHWGLINYGV
Motif3	68	-	GWMPKRGDFDYEWDDAEAEIADMEILEDDT PEEVELKLRLLLEIYNAKLDERERRKEFVLSRNLDFK
Motif4	44	Myb DNA-binding domain	RRRWTPPEDELLREAVAKYGAGDWARLAAEYLPGRGTGKQLRARW
Motif5	47	Zinc finger, ZZ type	IEYCCDCCGDDCSRLRYHCATCADMDLCPDCFSVGRYPSPHKARDFI
Motif6	35	-	HAQKYFLKVQKNKTGEYVPPRPKRRASSPYPRAA

Table 2. Cont.

Motifs	Width (aa)	Pfam ($p < 1 \times 10^{-5}$)	Sequences
Motif7	49	-	AGVAGAGAGGGGAAGGGGAAGAGGGG GGGGGGGGGGGGGGGGGGGGGGA
Motif8	82	DnaJ	KLTARNSDDLYELLELGDKRWHATEDDIKAFRRRLSLKYHPDKIA HAGEEAMEDAGEHFKAMRKAFDTLSDRRKRAAYDSID
Motif9	69	-	LGDENTPMEEVHAFYDFWYRFKSWRDFSADLEFDPEQADSR EERRWMDRQNAKHIKRRRAAEASRILL
Motif10	53	SWIRM-associated domain at the N-terminal	ATHIVYDPPPGTTEAETEGEDYCRALKRKG QVLVHWWYYPDSYDSWIPRQEV

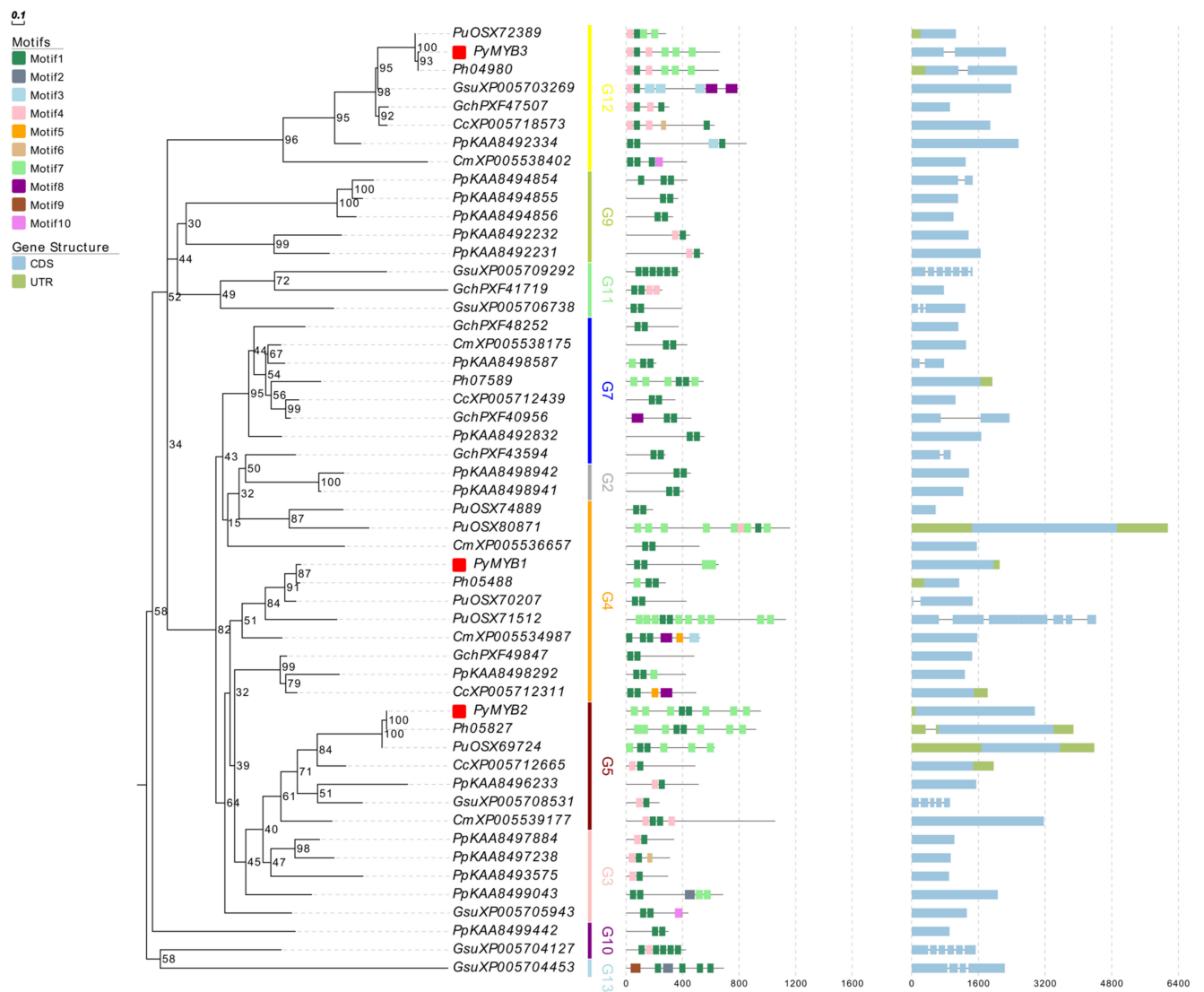


Figure 2. Phylogenetic (left) and conserved motif (middle) analyses and gene structures (right) of eight representative red algae R2R3-MYB genes. Red rectangles: R2R3-PyMYBs.

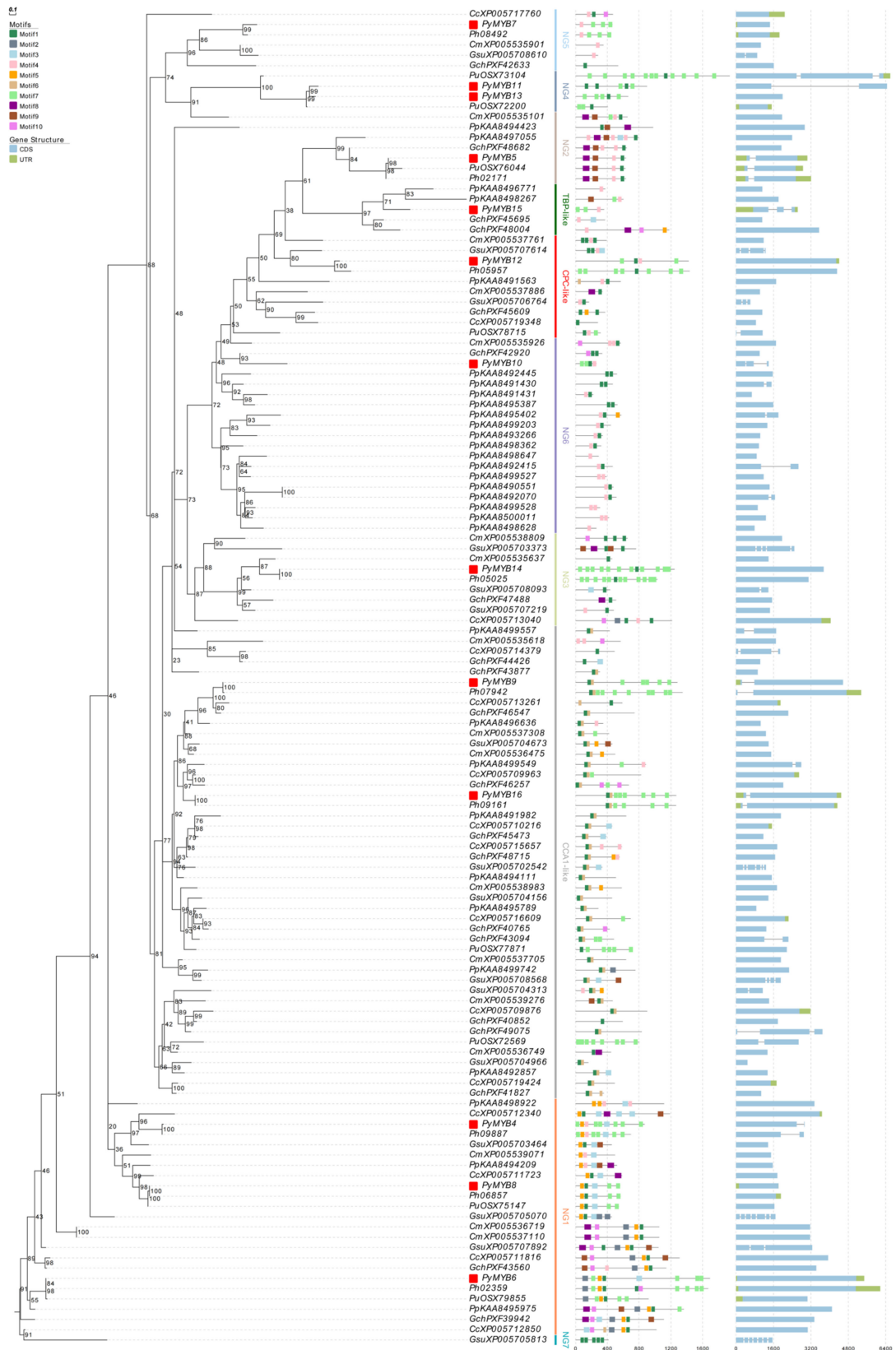


Figure 3. Phylogenetic (left) and conserved motif (middle) analyses and gene structures (right) of eight representative red algae MYB-related genes. Red rectangles: MYB-related *PyMYBs*.

A synteny analysis was performed between *Py. yezoensis* and other red algae species at the genome-wide level. Most *PyMYB* (13/16) genes had corresponding orthologous genes in other red algae species (Table S5) and mostly overlapped with the aforementioned gene pairs with similar motif compositions. Thirteen and five *PyMYB* genes were orthologous to the *MYB* genes in *Py. haitanensis* and *Po. umbilicalis*, respectively (Figure 4). No orthologous pairs were found in other red algae species pairs using MCScanX software (<https://github.com/wyp1125/MCScanX> accessed on 10 October 2023) or gene duplication identification criteria, which may have been caused by the long period of species divergence, leading to larger genetic differences. All identified collinear gene pairs exhibited Ka/Ks ratio values that were far less than one (Table S5), confirming that the evolution of the *MYB* gene family in the Bangiaceae family underwent a strong purifying selection.

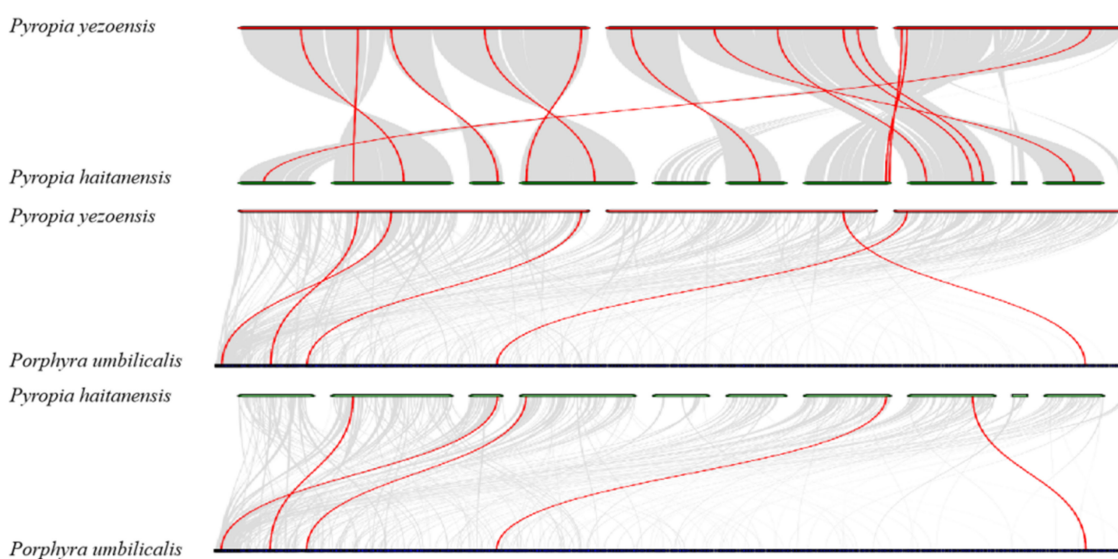


Figure 4. Synteny analysis of *Pyropia yezoensis*, *Pyropia haitanensis*, and *Porphyra umbilicalis*. Gray lines in the background indicate collinear blocks between two genomes, whereas red lines highlight syntenic *MYB* gene pairs.

No paralogous duplication events were found in the *PyMYB* genes of the *Py. yezoensis* genome. The same phenomenon also occurred in the other red algae species, except for *C. merolae* and *P. purpureum*, which both contained a pair of *MYB* paralogous genes (CmXP_005537110–CmXP_005536719 and PpKAA8490551–PpKAA8492070) (Figure 3).

2.4. Cis-Regulatory Element Analysis of the *PyMYB* Gene Family

Cis-elements can provide important insight into gene function prediction because they regulate gene expression. Therefore, we analyzed the *cis*-elements in the promoter regions of 16 *PyMYB* genes and explored the regulatory mechanisms of *PyMYB* genes in stress response and growth and development (Figure 5). A total of 28 *cis*-elements were identified and mainly grouped into four categories: growth and development, stress response, phytohormone response, and light response (Figure 5). The stress-responsive category accounted for the highest proportion (35.88%) among the four *cis*-element categories, which included ARE (anaerobic induction), DRE (dehydration, low temperature, and salt stress responsiveness), GC-motif (anoxic specific inducibility), LTR (low-temperature responsiveness), MBS (drought inducibility), and TC-rich repeats (defense and stress responsiveness). We found that 31.62% of these elements belonged to the phytohormone response category and were involved in ABA responsiveness (ABRE), auxin responsiveness (TGA element), gibberellin responsiveness (GARE and P-box), MeJA responsiveness (CGTCA motif and TGACG motif), and SA responsiveness (TCA element) (Figure 5). In the light response category, we also found that the ACE motifs, G-box, and Sp1 accounted for 29.31% of all elements (Figure 5). In the growth and development category, we identified four other

elements (CAT-box, MAS-like, NON-box, and O2-site), which accounted for 3.20% of all elements (Figure 5). According to these results, *PyMYB* genes participate in diverse functions including phytohormone response, stress response, light response, and plant growth and development.

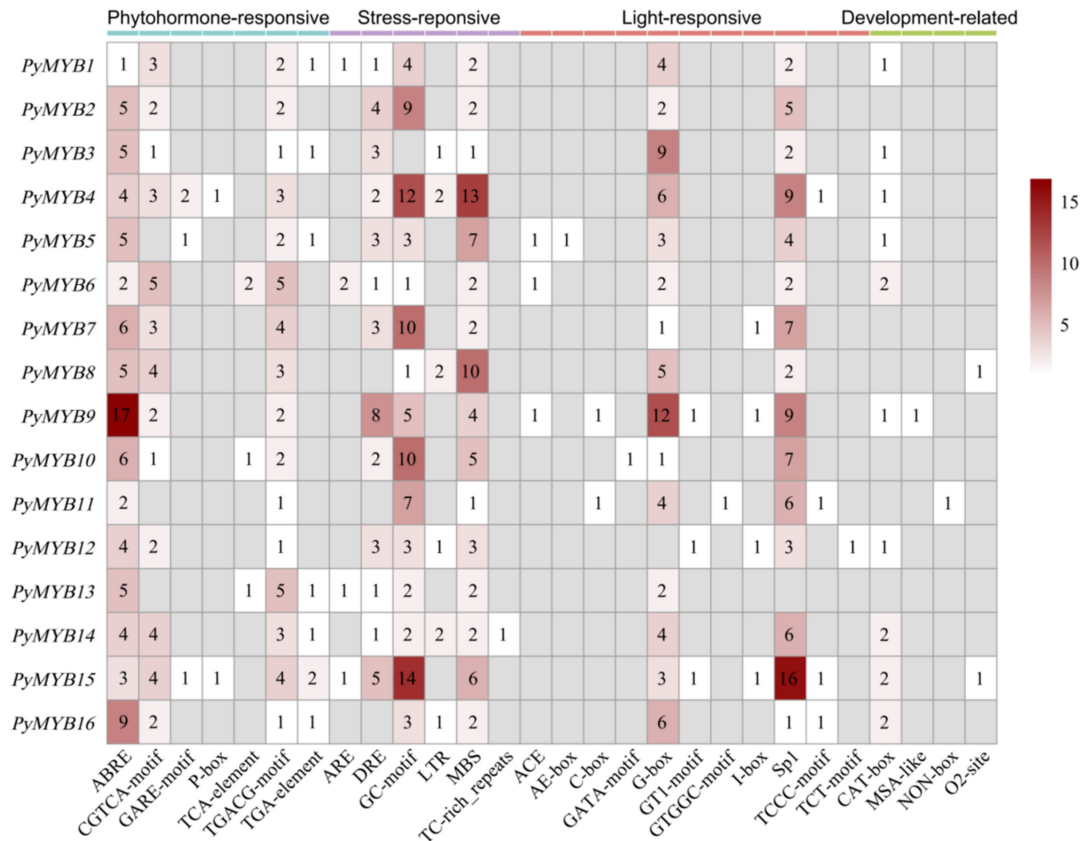


Figure 5. Analysis of 2-kb upstream *cis*-acting elements found in *PyMYB* genes. The different colors and numbers in the grid indicate the number of promoter elements.

2.5. Expression Patterns of *PyMYB* Genes in Different Life Stages and Blade Parts of *Py. yezoensis*

Py. yezoensis has a heteromorphic life cycle with two life cycle stages: gametophytic haploid blades (GAM) and sporophytic diploid filaments (conchocelis, SPO). The expression patterns of the 16 *PyMYB* genes in the two different life cycle stages are presented in Figure 6A. *PyMYB15* and *PyMYB16* exhibited the same expression pattern: high expression levels in GAM and low expression levels in SPO. The other *PyMYB* genes exhibited opposite expression patterns.

We also investigated the expression of *PyMYB* expression in the base of blades (BASE), spermatangium cells (SC), carposporangium cells (CC), and vegetative cells (VC) (Figure 6B,C). The primers of 10/16 *PyMYBs* were well designed, and we performed a quantitative real-time polymerase chain reaction (qRT-PCR) analysis; in contrast, the other six genes did not have suitable primers designed for qRT-PCR. These 10 genes were all highly expressed in SC and CC but maintained low or no expression in VC and BASE. However, these *PyMYB* genes exhibited different patterns in the two types of germ cells. *PyMYB3* and *PyMYB5* were relatively highly expressed in CC, whereas *PyMYB4*, *PyMYB7*, *PyMYB8*, *PyMYB9*, and *PyMYB16* were relatively highly expressed in SC.

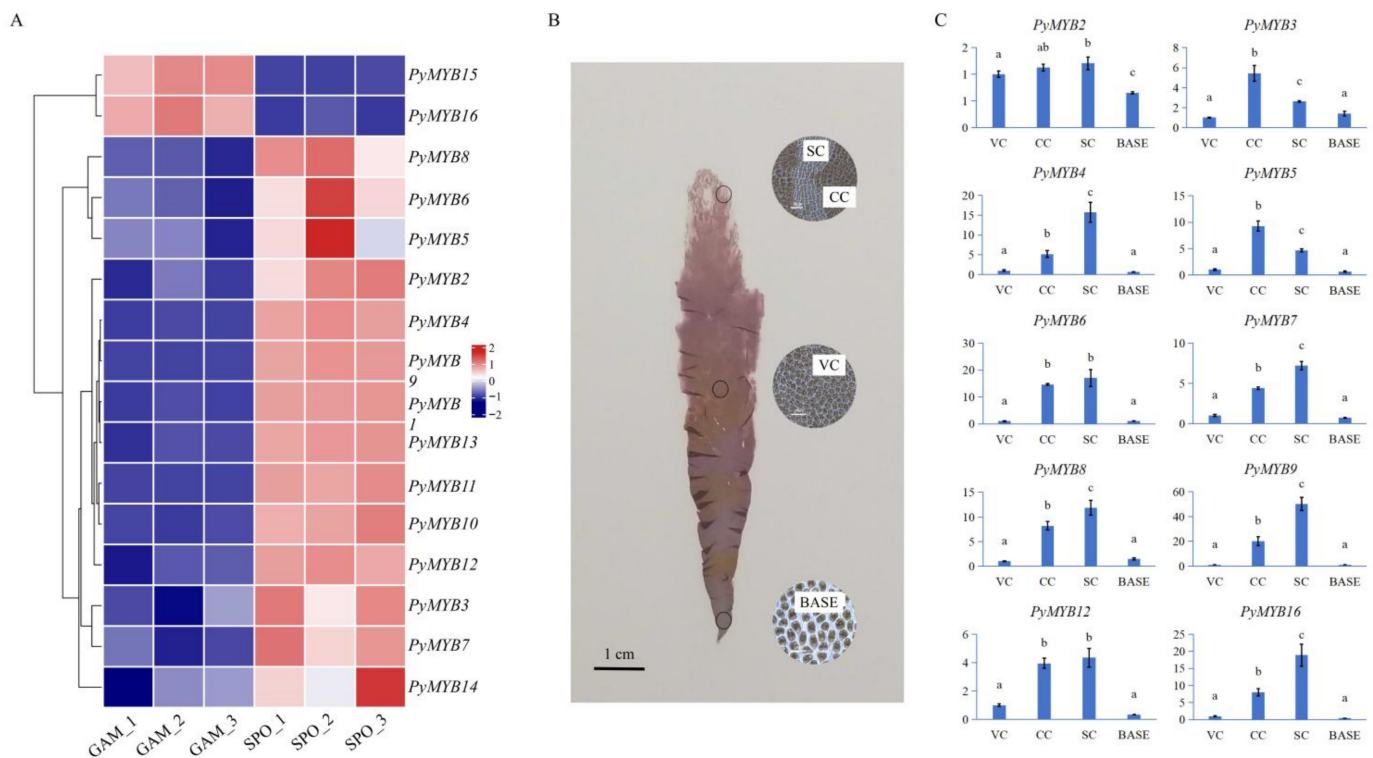


Figure 6. (A) Heatmap of the expression pattern of *PyMYB* genes in two life cycle stages: gametophytes (GAM) and sporophytes (SPO). The color bar (right) represents expression data after standardization on the row scale. (B) Four parts of *Py. zeoensis* blades. The micrograph in the circle has a scale of 20 μm . (C) Expression analysis of *PyMYBs* in different blade parts, as determined by qRT-PCR. The y -axis indicates the relative expression level, and the x -axis represents the different blade parts collected for expression analysis. The $2^{-\Delta\Delta\text{Ct}}$ method was used to calculate the relative gene expression values. Each data point represents the mean \pm standard deviation (SD) ($n = 3$). The lowercase letters on the bar chart represented the results of significance analysis ($p < 0.05$).

2.6. Expression Patterns of *PyMYB* Genes in Response to Biotic and Abiotic Stress

We investigated the expression patterns of *MYB* family members in *Py. zeoensis* in response to biotic and abiotic stress to further understand the impact of dehydration and rehydration, high and low temperatures, and red rot disease infection. In dehydration treatments (Figure 7A), *PyMYB3*, *PyMYB7*, and *PyMYB15* exhibited low expression to different degrees during dehydration and high expression during rehydration. The expression of the six *PyMYB* genes, namely *PyMYB1*, *PyMYB6*, *PyMYB10*, *PyMYB11*, *PyMYB13*, and *PyMYB16*, showed no obvious change at the beginning of dehydration stress, whereas their expression levels significantly decreased in severe dehydration treatment (absolute water content 20%, AWC20) and recovered in the rehydration treatment. *PyMYB2*, *PyMYB5*, and *PyMYB9* exhibited higher expression in severe dehydration treatment (AWC20) compared with other treatments. *PyMYB4*, *PyMYB8*, *PyMYB12*, and *PyMYB14* exhibited higher expression in the control treatment (AWC100) compared with the other treatments, indicating that these genes were downregulated under drought stress.

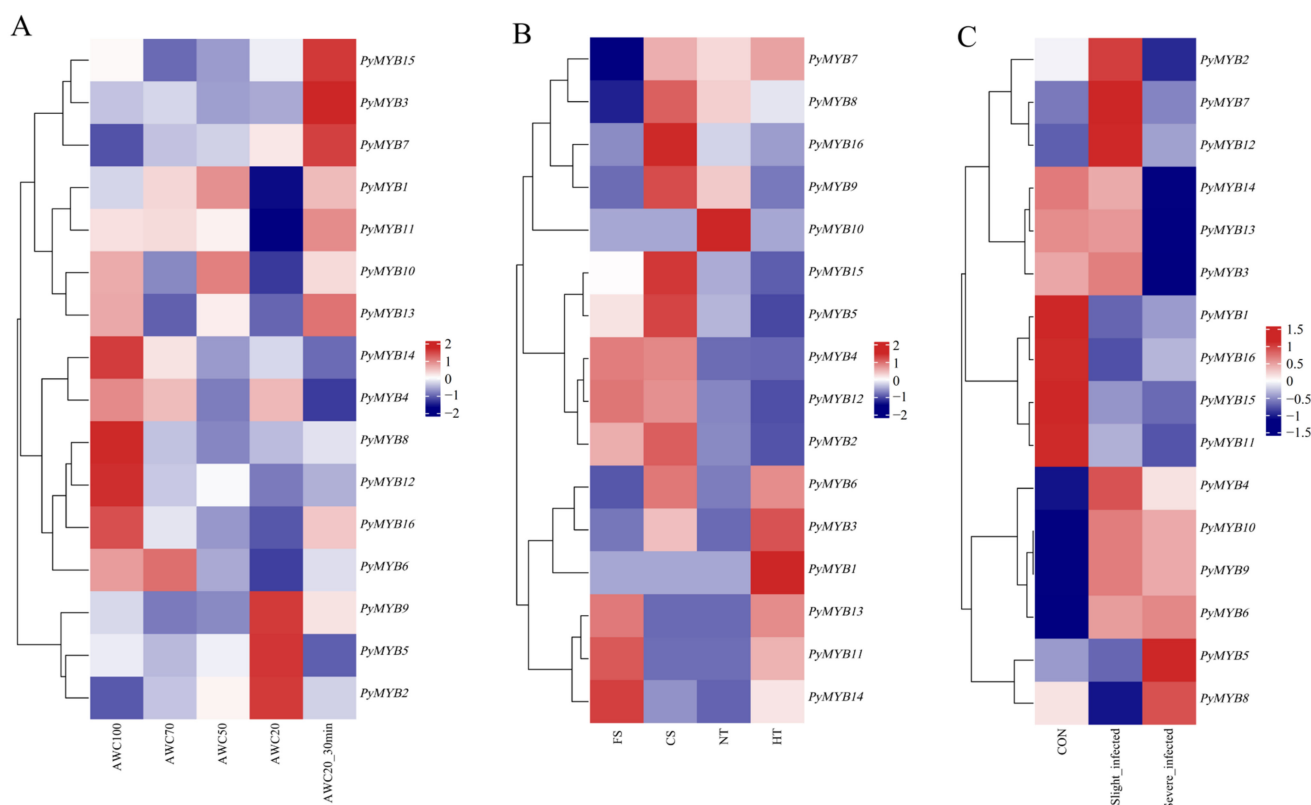


Figure 7. (A) Heatmap of the expression patterns of *PyMYB* genes in response to osmotic stress: absolute water content 100% (AWC100, control), absolute water content 70% (AWC70), absolute water content 50% (AWC50), absolute water content 20% (AWC20), and rehydrated 30 min after 20% of water loss (AWC20_30min). The color bar (right) represents log₂ expression levels (FPKM). (B) Heatmap of the expression patterns of *PyMYB* genes in response to temperature stress: normal temperature (NT, 8 °C), high temperature (HT, 24 °C), cold stress (CS, 0 °C), and freezing stress (FS, −8 °C). The color bar (right) represents log₂ expression levels (FPKM). (C) Heatmap of the expression patterns of the *PyMYB* genes in response to red rot disease. “CON” indicates the control (uninfected) area; “Slight_infected” and “Severe_infected” indicate two infected areas with different degrees. The color bar (right) represents expression data after standardization on the row scale.

We found different expression patterns in different genes as a result of temperature stress (Figure 7B). Compared with the normal temperature treatment (NT), the expression pattern of the *PyMYB* genes varied in response to high (HT), cold (CS), and freezing (FS) temperature stress. The majority exhibited higher expression under low temperatures (CS treatment or FS treatment) compared with NT and HT treatments, except for *PyMYB1*, *PyMYB3*, *PyMYB6*, *PyMYB7*, and *PyMYB10*. *PyMYB1* exhibited higher expression under HT treatment compared with the other temperature treatments. *PyMYB3* and *PyMYB6* exhibited higher expression under the CS and HT treatments compared with the other two temperature treatments. *PyMYB7* exhibited higher and a more stable expression under CS, NT, and HT treatments compared with FS treatment. *PyMYB10* exhibited higher expression under NT treatment but low expression under other temperature treatments.

The necrotrophic oomycete pathogen *Pythium porphyrae* causes red rot disease, which is lethal to the gametophytes of *Py. yezoensis*. These *PyMYB* genes exhibited significant specific expression under different infection levels (Figure 7C). *PyMYB1*, *PyMYB11*, *PyMYB15*, and *PyMYB16* exhibited high expression only in the control area (CON) but stable low expression in the other two infected areas. *PyMYB2*, *PyMYB7*, and *PyMYB12* exhibited high expression only in slightly infected areas, whereas *PyMYB5* and *PyMYB8* exhibited high expression only in severely infected areas. *PyMYB3*, *PyMYB13*, and *PyMYB14* exhibited high and a more stable expression in control areas and slightly infected areas but low

expression in severely infected areas. *PyMYB4*, *PyMYB6*, *PyMYB9*, and *PyMYB10* exhibited low expression in normal areas and high and a more stable expression in the other two infected areas.

3. Discussion

3.1. Evolution Analysis of MYB Genes in Red Algae

MYB TFs constitute one of the largest TF families in the plant kingdom [3]. In this study, we identified 16 MYB family genes in the *Py. yezoensis* genome, including 3 R2R3-MYBs and 13 MYB-related members. We also identified MYB genes in seven other red algae species, all of which exhibited significantly lower numbers when compared to higher plants [30,44]. The possible reasons for this difference included the following: red algae lineages underwent genome reduction in their last common ancestor [45,46], and paralogous duplication events were extremely rare in these red algae, although they occurred frequently in higher plants [14,47]. Similar results were also found in some Chlorophyta and Charophyta species with similarly simple organism structures (Table S2), which may be because higher plants generally require more genes to regulate complicated growth and biological processes [48].

Our analysis of phylogenetic relationships and consensus motifs supports the classification of red algae R2R3-MYB genes into 10 subgroups and red algae MYB-related genes into 10 subgroups. Most red algae MYB genes were clustered with green plants (G4, G5, G9, G10, G11, G12, CCA1-like/R-R-type, TBP-like, and CPC-like subgroups NG1, NG2, and NG4–NG6) or Glaucophyta species (G11, G12, G13, CCA1-like/R-R-type, TBP-like, and CPC-like subgroups NG2 and NG4). These genes were possibly formed in the ancestor of Archaeplastida. There were also some red algae-specific subgroups, such as G2, G3, G7, and NG3, indicating that these types of MYB genes may have been lost in other lineages in the very early stages of evolution.

Almost all MYB genes in Bangiaceae species, including *Py. yezoensis*, contain the Gly-rich motif (Motif7), which is absent in Florideophyceae species. This phenomenon was consistent with previous genome research in which it was found that Gly and Ala contained the least carbon atoms (two and three, respectively) and were enriched in Bangiales compared with Florideophyceae [39,49], indicating the evolutionary adaptation to carbon limitation and driving the high GC content evolution. However, a similar GC-rich motif has not been found in other studies of Bangiaceae red algae gene families [50,51]. The MYB genes in Bangiaceae species may have evolved directly in response to the effects of carbon limitation. The Gly-rich motif, which controls protein conformation, plays an essential role in the interaction with enzymes, substrates, and other types of non-covalent molecular binding [52,53] and is presumably involved in cold tolerance and acclimation development [54,55].

3.2. Functional Diversity of PyMYB Genes

Several biological processes, such as development, stress response, and hormone response, are controlled and regulated by the transcription of gene expression, which involves the molecular switches in *cis*-regulatory elements [56]. Therefore, to explore the functions of MYBs, *cis*-regulatory element predictions have been used extensively in several species [9,10]. The results of this study found various development-related, light-responsive, phytohormone-responsive, and stress-responsive elements in the promoter regions of *PyMYB* genes. For example, ABRE, which is involved in the ABA responsiveness of various stressors and plant growth and development [57], was present in all *PyMYB* promoter sequences. The DRE and LTR elements, which were both associated with various abiotic stressors, such as dehydration, low temperature, and salt stress [58,59], were also found in most of the *PyMYB* promoter sequences. As a result, *PyMYB* genes could regulate diverse development and stress-responsive processes.

Spatiotemporal regulation of the MYB gene family has been observed in various tissues and developmental stages [37,60–62]. Previous studies have shown that some MYB

genes play an essential role in germ cell specification by activating a germline-specific differentiation program [63]. For example, *Arabidopsis* male germline-specific MYB protein DUO1, as a positive regulator of male germline development, is required for correct male germ cell differentiation, division, and fertilization [64,65]; *MpFGMYB* has been proven to be a key regulator of female sexual differentiation in the haploid-dominant dioicous liverwort, and its loss resulted in female-to-male sex conversion [66]. *Py. yezoensis* is monocious, which means it can produce spermatangium cells and carposporangium cells in one thallus by cell differentiation. In our study, most *PyMYB* genes exhibited significantly high expression in the two types of germ cells compared with vegetative and basal cells, indicating that they played an essential role in cell differentiation. However, the different expression patterns of these genes in the two types of germ cells further suggested that they might play different roles during cell differentiation. *MYB* expression differentiation was found in plant life cycles that alternate between haploid gametophytes (in which male and female gametes are produced) and diploid sporophytes (in which haploid spores are produced through meiosis) [67,68]. The haploid–diploid heteromorphic life cycle of *Py. yezoensis* features a diploid microscopic filamentous sporophyte and a haploid macroscopic blade-forming gametophyte [39]. The results of our study showed the spatiotemporal regulation of the *PyMYB* genes in different life cycle stages of *Py. yezoensis*. Some of the *PyMYB* genes were highly expressed in sporophytes, while others were highly expressed in gametophytes. How these *PyMYBs* performed during development revealed that *Py. yezoensis* regulated the expression of *PyMYB* genes by developing a sophisticated mechanism when and where required.

Major abiotic stressors that can affect the development and growth of laver under various intertidal conditions include dehydration and temperature changes [39]. *MYB* TFs function as key mediators of various stress responses through complex activities, including ABA and other multiple stress signaling pathways [29,69,70] and many other cellular processes [71]. For example, the overexpression of *LIMYB3* in *A. thaliana* L. transgenic plants revealed ABA hypersensitivity and enhanced tolerance to cold, drought, and salt stress [72]. Another experiment on the overexpression of *CmMYB2* yielded similar results [73]. Some *MYB* genes can control secondary wall thickening and participate in stress responses [21,74]. *Py. yezoensis* is an ideal and attractive model for studying the molecular mechanisms of stress resistance because of the complexity of its intertidal living environment and its economic value [39]. In this study, the expression profiles of *PyMYB* genes under biotic (red rot disease infection) and abiotic (dehydration/rehydration and high/low temperature) stress showed that several *MYB* genes were induced significantly and revealed differential expression patterns. These results indicated that different *PyMYB* genes may affect the response to biotic and abiotic stress. For example, *PyMYB2*, *PyMYB5*, and *PyMYB9* responded to dehydration and low temperature by elevating their expression levels, which means that they are closely associated with various abiotic stressors. *PyMYB5* was also upregulated after *Pythium porphyrae* infection, indicating that this gene plays an essential role in the red rot disease response and tolerance and can be used as a candidate gene for future genetic improvement. These results support further functional exploration.

4. Materials and Methods

4.1. Identification and Characteristics of MYB Genes in *Py. yezoensis*

To identify the *MYB* gene family members in *Py. yezoensis*, we followed two approaches. First, all of the known *Arabidopsis* *MYB* gene sequences were used as queries to perform multiple database searches against the protein and genome files downloaded from the *Py. yezoensis* database (<https://www.ncbi.nlm.nih.gov/bioproject/PRJNA589917>, accessed on 6 September 2022) [39]. The *MYB* genes of *Arabidopsis thaliana* were obtained from online published work and further used in the following phylogenetic analysis [44]. Stand-alone versions of the Basic Local Alignment Search Tool (<http://blast.ncbi.nlm.nih.gov>, accessed on 6 September 2022) were used, with an e-value cutoff of 1×10^{-5} . Second, the hidden Markov model profile for the *MYB*-binding domain (PF00249) was

downloaded from the Pfam database (<http://pfam.xfam.org/>, accessed on 7 September 2022) and used as a query to search the *Py. yezoensis* database using HMMER 3.1 (<http://hmmer.org/download.html>, accessed on 7 September 2022) with a cutoff value of 0.01. Two more steps were performed to confirm the accuracy of the domains. First, the SMART website (<http://smart.embl-heidelberg.de>, accessed on 8 September 2022), NCBI-CDD (<http://www.ncbi.nlm.nih.gov/Structure/cdd/wrpsb.cgi>, accessed on 8 September 2022), and InterProScan (<http://www.ebi.ac.uk/interpro/result/InterProScan/>, accessed on 8 September 2022) were used to confirm the obtained MYB protein sequences. Then, GARP-like TFs, which contain a consensus sequence (SHLQKY) and are often confused with MYB-related CCA1-like proteins (SHAQK(Y/F)F), should be further removed [37]. GARP-like TFs contain only one of the three regularly spaced Trp residues in the MYB domain. Thus, MYB domains with more than two conserved Trp residues mutated were manually removed to exclude GARP proteins [37,44,47].

All non-redundant *Py. yezoensis* MYB genes were classified into different types (R2R3, MYB-related) by manually inspecting the number of MYB-binding domains and were named first by their category (R2R3 and MYB-related) and then by genomic location. With the use of the same method described above, MYB genes were also identified in seven other red algae species (*Pyropia haitanensis* [42], *Porphyra umbilicalis* [75], *Chondrus crispus* [76], *Cyanidioschyzon merolae* [77], *Gracilariopsis chorda* [78], *Porphyridium purpureum* [79], and *Galdieria sulphuraria* [80]), three green algae species (*Chlamydomonas reinhardtii* (NCBI accession: GCF_000002595.1), *Micromonas pusilla* (GCF_000151265.2), and *Chara braunii* (GCA_003427395.1), and one Glaucophyta species (*Cyanophora paradoxa* [81]), which are well-studied and evolutionarily important representative species.

We obtained gene structure information of the *PyMYB* genes from the *Py. yezoensis* genome database and displayed it using EVOLVIEW (<https://www.evolgenius.info/evolview/>, accessed on 10 April 2023). To obtain the protein MW and pI of each *PyMYB* gene, we used ExpASy [82]. The conserved motifs of the *PyMYB* protein sequences and seven other red algae species' MYB protein sequences were predicted using MEME (<http://meme-suite.org/tools/meme>, accessed on 10 April 2023) with the following parameters: an optimum motif width of ≥ 35 and ≤ 100 and a maximum number of motifs of 10 [83].

4.2. Phylogenetic Analysis of MYB Proteins

We retrieved the amino acid sequences of the MYB-binding domains (R repeats) from each MYB protein sequence and conducted multiple sequence alignments using MUSCLE (v 3.8.425) [84]. The phylogenetic trees of R2R3-MYB and MYB-related genes were reconstructed with the maximum likelihood (ML) using IQ-TREE multicore version 2.2.2.3 software [85] (parameter: $-\text{bb } 1000 -\text{TEST}$). For each reconstruction, we used the $-\text{TEST}$ parameter to select the best model and completed 1000 ultrafast bootstraps. We also inferred ML phylogenies for 13 representative species from different taxonomic groups using FastTree (<http://www.microbesonline.org/fasttree/>, accessed on 17 April 2023).

4.3. Gene Synteny and Duplication for MYB Genes

We used MCScanX software (<https://github.com/wyp1125/MCScanX>, accessed on 10 October 2022) to perform a microsynteny analysis of *Py. yezoensis* and other red algae species [86]. To analyze potential gene duplications, we used the following criteria: (1) the similarity of the aligned gene regions was $\geq 70\%$ and (2) the sequence alignment covered $\geq 70\%$ of the longer gene [87]. For each duplicated gene pair, we calculated nonsynonymous (Ka) substitution and synonymous (Ks) substitution using the KaKs_Calculator [88].

4.4. Cis-Regulatory Element Analysis of *PyMYB*s

We extracted sequences in the 2000 base pairs (bp) upstream of the start codon (ATG) in the MYB genes from the genome of *Py. yezoensis*. For promoter *cis*-acting regulatory element screening, we analyzed the sequences extracted above using the PlantCARE

database (<http://bioinformatics.psb.ugent.be/webtools/plantcate/html>, accessed on 6 November 2022) [89].

4.5. Expression Profile Analysis

The transcriptome data of two life cycle stages in *Py. yezoensis* (gametophyte and sporophyte; NCBI SRA: SRR10527930–SRR10527937), osmotic stress (dehydration/rehydration; NCBI BioProject: PRJNA401507), temperature stress (hot/cold/freezing; NCBI BioProject: PRJNA235353), and red rot disease (*Pythium porphyrae* infection; NCBI BioProject: PRJNA560692) conditions of *Py. yezoensis* were obtained from previously published studies [39–41,90]. We used FastQC [91] and Trimmomatic [92] to evaluate the quality and trim the low-quality raw sequencing reads. We performed differential gene and transcript expression analyses of the RNA-sequencing experiments using TopHat and Cufflinks [93]. All fragments, per kilobase of transcript per million fragments mapped (FPKM) values of gene expression, were standardized on the row scale and clustered and visualized with TBtools [94]. Genes with low expression levels (FPKM <2) were filtered.

4.6. RNA Isolation and qRT-PCR Analysis

The blades of *Py. yezoensis* used in the experiment were obtained from a farm in Rizhao Lanshan, China. The collected materials were cultured in bubbling natural seawater with Provasoli's enrichment solution medium with 50 $\mu\text{mol photons m}^{-2}\cdot\text{s}^{-1}$ at 8 ± 1 °C and a 12:12 light:dark photoperiod for 3 days under laboratory conditions. When the blades entered the mature period, different parts of the blades (e.g., the base of blades, spermatangium cells, carposporangium cells, and vegetative cells) were segmented and selected under an anatomical microscope and confirmed under an optical microscope (Figure 6B). For each treatment, we set three biological replicates and collected and placed the samples in liquid nitrogen for RNA isolation. We used the RNeasy Plant Mini Kit (OMEGA) to extract the total RNA according to the manufacturer's instructions. We used about 1 μg of total RNA to synthesize the first-strand cDNA using a HiScript[®] III RT SuperMix for qPCR (+gDNA wiper) Kit (Vazyme Biotech Co., Ltd., Nanjing, China). We performed qRT-PCR following previous work [95]. We used the Light-Cycle[®] 480 Real-Time PCR System to verify the selected genes according to the following cycling conditions: 95 °C for 90 s, followed by 40 cycles of 95 °C for 5 s, 60 °C for 15 s, and 72 °C for 20 s. The reference genes were cystathionine gamma-synthase 1 (CGS1) and ubiquitin-conjugating enzyme (UBC) genes [96]. Supplementary Table S1 lists the primer sequences. The $2^{-\Delta\Delta\text{Ct}}$ method was used to calculate the relative gene expression values using R 3.6.0 software. The significance of differences was analyzed using the R package "ggsignif" ($p < 0.05$).

5. Conclusions

In this study, we performed genome-wide identification and analysis of MYB genes encoded in the *Py. yezoensis* genome and identified 3 R2R3-MYBs and 13 MYB-related genes. The phylogenetic analysis suggested *PyMYBs*' ancient origin and no trace of gene duplication events. Considering the other red algae MYB gene information, we inferred that the Bangiaceae-only Gly-rich motif might be linked to evolutionary adaptation. We also conducted an expression analysis of *PyMYB* genes in different developmental stages and stress conditions and found that the MYB family had a wide expression profile and played essential roles in growth, dehydration, temperature, and disease stress responses. *PyMYB2*, *PyMYB5*, and *PyMYB9* responded to dehydration and low temperatures through elevated expression levels, indicating that they are closely associated with various abiotic stressors. *PyMYB5* was also upregulated after *Pythium porphyrae* infection, indicating that this gene plays an essential role in the red rot disease response and tolerance and can be used as a candidate gene for future genetic improvement. Our results provide new insights into the potential role of MYB TFs in specific developmental transitions and stress responses in *Py. yezoensis*, thus laying the foundation for further functional investigations of *PyMYB* genes.

Supplementary Materials: The following supporting information can be downloaded at: <https://www.mdpi.com/article/10.3390/plants12203613/s1>, Figure S1: Maximum likelihood (ML) tree of *R2R3-MYB* genes in 13 species using IQ-TREE software; Figure S2: Maximum likelihood (ML) tree of *R2R3-MYB* genes in 13 species using FastTree software; Figure S3: Maximum likelihood (ML) tree of *MYB*-related genes in 13 species using IQ-TREE software; Figure S4: Maximum likelihood (ML) tree of *MYB*-related genes in 13 species using FastTree software; Table S1: Gene primers designed for qRT-PCR; Table S2: Number of *MYB* genes in the examined species; Table S3: The *MYB* gene IDs of *MYB* genes in the examined species; Table S4: Multiple sequence alignment used to infer phylogenetic trees Table S5: Ka, Ks and Ka/Ks values for duplicated ortholog pairs in *Py. jezoensis* and *Py. haitanensis*/*Po. umbilicalis*.

Author Contributions: Y.M. and X.Y. arranged and designed the study. X.Y. analyzed the data, performed the experiments, and wrote the first draft. L.T. and X.T. completed the visualization of the data. L.T., X.T. and Y.M. revised the manuscript. All authors have read and agreed to the published version of the manuscript.

Funding: The authors thank the grants supporting from the National Natural Science Foundation of China (Grant No. 32060829), National Key R&D Program of China (2020YFD0901101), China Postdoctoral Science Foundation (2021M703033), the 2020 Research Program of Sanya Yazhou Bay Science and Technology City (No. SKJC-2020-02-009), the Innovation Platform for Academicians of Hainan Province, the Major Science and Technology Program of Yazhou Bay Innovation Institute of Hainan Tropical Ocean University (2022CXZYD001), the 2023 Provincial Key Discipline Construction Project of Hainan Tropical Ocean University (46000023T000000946867), National Natural Science Foundation of China (42306116), and the Qingdao Postdoctoral Applied Research Project (2020).

Data Availability Statement: All datasets generated in this study are included as Supplementary Materials of this article.

Acknowledgments: We are very grateful to Yunxiang Mao for his guidance. We thank the Key Laboratory of Marine Genetics and Breeding (Ocean University of China), Key Laboratory of Utilization and Conservation of Tropical Marine Bioresource (Hainan Tropical Ocean University), and lab members for their assistance in this study.

Conflicts of Interest: The authors declare no conflict of interest.

References

1. Moreira, D.; Le Guyader, H.; Philippe, H. The origin of red algae and the evolution of chloroplasts. *Nature* **2000**, *405*, 69–72. [CrossRef]
2. Mumford, T.; Miura, A. Porphyra as food: Cultivation and economics. In *Algae and Human Affairs*; Cambridge University Press: Cambridge, UK, 1988; pp. 87–118.
3. Wang, H.; Wang, H.; Shao, H.; Tang, X. Recent advances in utilizing transcription factors to improve plant abiotic stress tolerance by transgenic technology. *Front. Plant Sci.* **2016**, *7*, 67. [CrossRef]
4. Dubos, C.; Stracke, R.; Grotewold, E.; Weisshaar, B.; Martin, C.; Lepiniec, L. *MYB* transcription factors in *Arabidopsis*. *Trends Plant Sci.* **2010**, *15*, 573–581. [CrossRef]
5. Sun, W.; Ma, Z.; Chen, H.; Liu, M. *MYB* gene family in potato (*Solanum tuberosum* L.): Genome-wide identification of hormone-responsive reveals their potential functions in growth and development. *Int. J. Mol. Sci.* **2019**, *20*, 4847. [CrossRef]
6. Paz-Ares, J.; Ghosal, D.; Wienand, U.; Peterson, P.; Saedler, H. The regulatory *c1* locus of *Zea mays* encodes a protein with homology to *MYB* proto-oncogene products and with structural similarities to transcriptional activators. *EMBO J.* **1987**, *6*, 3553–3558. [CrossRef]
7. Lin, B.L.; Wang, J.S.; Liu, H.C.; Chen, R.W.; Meyer, Y.; Barakat, A.; Delseny, M. Genomic analysis of the *Hsp70* superfamily in *Arabidopsis thaliana*. *Cell Stress Chaperones* **2001**, *6*, 201–208. [CrossRef] [PubMed]
8. Jia, L.; Clegg, M.T.; Jiang, T. Evolutionary dynamics of the DNA-binding domains in putative *R2R3-MYB* genes identified from rice subspecies *indica* and *japonica* genomes. *Plant Physiol.* **2004**, *134*, 575–585. [CrossRef]
9. Ai, P.; Xue, J.; Shi, Z.; Liu, Y.; Li, Z.; Li, T.; Zhao, W.; Khan, M.A.; Kang, D.; Wang, K.; et al. Genome-wide characterization and expression analysis of *MYB* transcription factors in *Chrysanthemum nankingense*. *BMC Plant Biol.* **2023**, *23*, 140. [CrossRef] [PubMed]
10. Si, Z.; Wang, L.; Ji, Z.; Zhao, M.; Zhang, K.; Qiao, Y. Comparative analysis of the *MYB* gene family in seven *Ipomoea* species. *Front. Plant Sci.* **2023**, *14*, 1155018. [CrossRef] [PubMed]
11. Liu, M.; Li, K.; Sheng, S.; Wang, M.; Hua, P.; Wang, Y.; Chen, P.; Wang, K.; Zhao, M.; Wang, Y.; et al. Transcriptome analysis of *MYB* transcription factors family and *PgMYB* genes involved in salt stress resistance in *Panax ginseng*. *BMC Plant Biol.* **2022**, *22*, 479. [CrossRef]

12. Xu, Q.; He, J.; Dong, J.; Hou, X.; Zhang, X. Genomic survey and expression profiling of the MYB gene family in watermelon. *Hortic. Plant J.* **2018**, *4*, 1–15. [[CrossRef](#)]
13. Abbas, F.; Ke, Y.; Zhou, Y.; Yu, Y.; Waseem, M.; Ashraf, U.; Wang, C.; Wang, X.; Li, X.; Yue, Y.; et al. Genome-wide analysis reveals the potential role of MYB transcription factors in floral scent formation in *Hedychium coronarium*. *Front. Plant Sci.* **2021**, *12*, 623742. [[CrossRef](#)]
14. Du, H.; Yang, S.-S.; Liang, Z.; Feng, B.-R.; Liu, L.; Huang, Y.-B.; Tang, Y.-X. Genome-wide analysis of the MYB transcription factor superfamily in soybean. *BMC Plant Biol.* **2012**, *12*, 106. [[CrossRef](#)] [[PubMed](#)]
15. Abdullah-Zawawi, M.-R.; Ahmad-Nizammuddin, N.-F.; Govender, N.; Harun, S.; Mohd-Assaad, N.; Mohamed-Hussein, Z.-A. Comparative genome-wide analysis of WRKY, MADS-box and MYB transcription factor families in *Arabidopsis* and rice. *Sci. Rep.* **2021**, *11*, 19678. [[CrossRef](#)]
16. Stracke, R.; Werber, M.; Weisshaar, B. The R2R3-MYB gene family in *Arabidopsis thaliana*. *Curr. Opin. Plant Biol.* **2001**, *4*, 447–456. [[CrossRef](#)] [[PubMed](#)]
17. Haga, N.; Kato, K.; Murase, M.; Araki, S.; Kubo, M.; Demura, T.; Suzuki, K.; Müller, I.; Voß, U.; Jürgens, G. R1R2R3-MYB proteins positively regulate cytokinesis through activation of KNOLLE transcription in *Arabidopsis thaliana*. *Development* **2007**, *134*, 1101–1110. [[CrossRef](#)]
18. Rosinski, J.A.; Atchley, W.R. Molecular evolution of the MYB family of transcription factors: Evidence for polyphyletic origin. *J. Mol. Evol.* **1998**, *46*, 74–83. [[CrossRef](#)]
19. Jiang, C.; Gu, J.; Chopra, S.; Gu, X.; Peterson, T. Ordered origin of the typical two-and three-repeat MYB genes. *Genetics* **2004**, *326*, 13–22. [[CrossRef](#)]
20. Huang, W.; Sun, W.; Lv, H.; Xiao, G.; Zeng, S.; Wang, Y. Isolation and molecular characterization of thirteen R2R3-MYB transcription factors from *Epimedium sagittatum*. *Int. J. Mol. Sci.* **2013**, *14*, 594–610. [[CrossRef](#)]
21. Guo, H.; Wang, Y.; Wang, L.; Hu, P.; Wang, Y.; Jia, Y.; Zhang, C.; Zhang, Y.; Zhang, Y.; Wang, C.; et al. Expression of the MYB transcription factor gene *BplMYB46* affects abiotic stress tolerance and secondary cell wall deposition in *Betula platyphylla*. *Plant Biotechnol. J.* **2017**, *15*, 107–121. [[CrossRef](#)] [[PubMed](#)]
22. Cao, Y.; Jia, H.; Xing, M.; Jin, R.; Grierson, D.; Gao, Z.; Sun, C.; Chen, K.; Xu, C.; Li, X. Genome-wide analysis of MYB gene family in Chinese bayberry (*Morella rubra*) and identification of members regulating flavonoid biosynthesis. *Front. Plant Sci.* **2021**, *12*, 691384. [[CrossRef](#)] [[PubMed](#)]
23. Vaillau, F.; Daniel, X.; Tronchet, M.; Montillet, J.-L.; Triantaphylides, C.; Roby, D. A R2R3-MYB gene, *AtMYB30*, acts as a positive regulator of the hypersensitive cell death program in plants in response to pathogen attack. *Proc. Natl. Acad. Sci. USA* **2002**, *99*, 10179–10184. [[CrossRef](#)] [[PubMed](#)]
24. Wang, X.; Niu, Q.-W.; Teng, C.; Li, C.; Mu, J.; Chua, N.-H.; Zuo, J. Overexpression of PGA37/MYB118 and MYB115 promotes vegetative-to-embryonic transition in *Arabidopsis*. *Cell Res.* **2009**, *19*, 224. [[CrossRef](#)]
25. Simon, M.; Lee, M.M.; Lin, Y.; Gish, L.; Schiefelbein, J. Distinct and overlapping roles of single-repeat MYB genes in root epidermal patterning. *Dev. Biol.* **2007**, *311*, 566–578. [[CrossRef](#)]
26. Kasahara, R.D.; Portereiko, M.F.; Sandaklie-Nikolova, L.; Rabiger, D.S.; Drews, G.N. MYB98 is required for pollen tube guidance and synergid cell differentiation in *Arabidopsis*. *Plant Cell* **2005**, *17*, 2981–2992. [[CrossRef](#)]
27. Baumann, K.; Perez-Rodriguez, M.; Bradley, D.; Venail, J.; Bailey, P.; Jin, H.; Koes, R.; Roberts, K.; Martin, C. Control of cell and petal morphogenesis by R2R3 MYB transcription factors. *Development* **2007**, *134*, 1691–1701. [[CrossRef](#)]
28. Jung, C.; Seo, J.S.; Han, S.W.; Koo, Y.J.; Kim, C.H.; Song, S.I.; Nahm, B.H.; Do Choi, Y.; Cheong, J.-J. Overexpression of *AtMYB44* enhances stomatal closure to confer abiotic stress tolerance in transgenic *Arabidopsis*. *Plant Physiol.* **2008**, *146*, 623–635. [[CrossRef](#)] [[PubMed](#)]
29. He, Y.; Li, W.; Lv, J.; Jia, Y.; Wang, M.; Xia, G. Ectopic expression of a wheat MYB transcription factor gene, *TaMYB73*, improves salinity stress tolerance in *Arabidopsis thaliana*. *J. Exp. Bot.* **2011**, *63*, 1511–1522. [[CrossRef](#)] [[PubMed](#)]
30. Chang, X.; Xie, S.; Wei, L.; Lu, Z.; Chen, Z.-H.; Chen, F.; Lai, Z.; Lin, Z.; Zhang, L. Origins and stepwise expansion of R2R3-MYB transcription factors for the terrestrial adaptation of plants. *Front. Plant Sci.* **2020**, *11*, 575360. [[CrossRef](#)]
31. Wu, W.; Zhu, S.; Zhu, L.; Wang, D.; Liu, Y.; Liu, S.; Zhang, J.; Hao, Z.; Lu, Y.; Cheng, T.; et al. Characterization of the *Liriodendron chinense* MYB gene family and its role in abiotic stress response. *Front. Plant Sci.* **2021**, *12*, 641280. [[CrossRef](#)] [[PubMed](#)]
32. Onkokesung, N.; Reichelt, M.; van Doorn, A.; Schuurink, R.C.; van Loon, J.J.A.; Dicke, M. Modulation of flavonoid metabolites in *Arabidopsis thaliana* through overexpression of the MYB75 transcription factor: Role of kaempferol-3,7-dirhamnoside in resistance to the specialist insect herbivore *Pieris brassicae*. *J. Exp. Bot.* **2014**, *65*, 2203–2217. [[CrossRef](#)]
33. Tang, Y.; Bao, X.; Zhi, Y.; Wu, Q.; Guo, Y.; Yin, X.; Zeng, L.; Li, J.; Zhang, J.; He, W.; et al. Overexpression of a MYB family gene, *OsMYB6*, increases drought and salinity stress tolerance in transgenic rice. *Front. Plant Sci.* **2019**, *10*, 168. [[CrossRef](#)]
34. Luo, Q.; Liu, R.; Zeng, L.; Wu, Y.; Jiang, Y.; Yang, Q.; Nie, Q. Isolation and molecular characterization of *NtMYB4a*, a putative transcription activation factor involved in anthocyanin synthesis in tobacco. *Gene* **2020**, *760*, 144990. [[CrossRef](#)]
35. Dubos, C.; Le Gourrierc, J.; Baudry, A.; Huep, G.; Lanet, E.; Debeaujon, I.; Routaboul, J.M.; Alboresi, A.; Weisshaar, B.; Lepiniec, L. MYB2 is a new regulator of flavonoid biosynthesis in *Arabidopsis thaliana*. *Plant J.* **2008**, *55*, 940–953. [[CrossRef](#)]
36. Tominaga-Wada, R.; Nukumizu, Y. Expression analysis of an R3-Type MYB transcription factor CPC-LIKE MYB4 (*TRICHOMELESS2*) and *CPL4*-related transcripts in *Arabidopsis*. *Int. J. Mol. Sci.* **2012**, *13*, 3478–3491. [[CrossRef](#)]

37. Du, H.; Wang, Y.-B.; Xie, Y.; Liang, Z.; Jiang, S.-J.; Zhang, S.-S.; Huang, Y.-B.; Tang, Y.-X. Genome-wide identification and evolutionary and expression analyses of MYB-related genes in land plants. *DNA Res.* **2013**, *20*, 437–448. [[CrossRef](#)] [[PubMed](#)]
38. Blouin, N.A.; Brodie, J.A.; Grossman, A.C.; Xu, P.; Brawley, S.H. *Porphyra*: A marine crop shaped by stress. *Trends Plant Sci.* **2011**, *16*, 29–37. [[CrossRef](#)] [[PubMed](#)]
39. Wang, D.; Yu, X.; Xu, K.; Bi, G.; Cao, M.; Zelzion, E.; Fu, C.; Sun, P.; Liu, Y.; Kong, F.; et al. *Pyropia yezoensis* genome reveals diverse mechanisms of carbon acquisition in the intertidal environment. *Nat. Commun.* **2020**, *11*, 4028. [[CrossRef](#)] [[PubMed](#)]
40. Sun, P.; Tang, X.; Bi, G.; Xu, K.; Kong, F.; Mao, Y. Gene expression profiles of *Pyropia yezoensis* in response to dehydration and rehydration stresses. *Mar. Genom.* **2019**, *43*, 43–49. [[CrossRef](#)]
41. Sun, P.; Mao, Y.; Li, G.; Cao, M.; Kong, F.; Wang, L.; Bi, G. Comparative transcriptome profiling of *Pyropia yezoensis* (Ueda) M.S. Hwang & H.G. Choi in response to temperature stresses. *BMC Genom.* **2015**, *16*, 463.
42. Cao, M.; Xu, K.; Yu, X.; Bi, G.; Liu, Y.; Kong, F.; Sun, P.; Tang, X.; Du, G.; Ge, Y.; et al. A chromosome-level genome assembly of *Pyropia haitanensis* (Bangiales, Rhodophyta). *Mol. Ecol. Resour.* **2020**, *20*, 216–227. [[CrossRef](#)]
43. Yang, X.; Guo, T.; Li, J.; Chen, Z.; Guo, B.; An, X. Genome-wide analysis of the MYB-related transcription factor family and associated responses to abiotic stressors in *Populus*. *Int. J. Biol. Macromol.* **2021**, *191*, 359–376. [[CrossRef](#)] [[PubMed](#)]
44. Chen, Y.; Yang, X.; He, K.; Liu, M.; Li, J.; Gao, Z.; Lin, Z.; Zhang, Y.; Wang, X.; Qiu, X. The MYB transcription factor superfamily of *Arabidopsis*: Expression analysis and phylogenetic comparison with the rice MYB family. *Plant Mol. Biol.* **2006**, *60*, 107–124.
45. Qiu, H.; Price, D.C.; Yang, E.C.; Yoon, H.S.; Bhattacharya, D. Evidence of ancient genome reduction in red algae (Rhodophyta). *J. Phycol.* **2015**, *51*, 624–636. [[CrossRef](#)] [[PubMed](#)]
46. Bhattacharya, D.; Qiu, H.; Lee, J.; Su Yoon, H.; Weber, A.P.M.; Price, D.C. When less is more: Red algae as models for studying gene loss and genome evolution in eukaryotes. *Crit. Rev. Plant Sci.* **2018**, *37*, 81–99. [[CrossRef](#)]
47. Pu, X.; Yang, L.; Liu, L.; Dong, X.; Chen, S.; Chen, Z.; Liu, G.; Jia, Y.; Yuan, W.; Liu, L. Genome-wide analysis of the MYB transcription factor superfamily in *Physcomitrella patens*. *Int. J. Mol. Sci.* **2020**, *21*, 975. [[CrossRef](#)]
48. Wu, Z.-J.; Li, X.-H.; Liu, Z.-W.; Li, H.; Wang, Y.-X.; Zhuang, J. Transcriptome-wide identification of *Camellia sinensis* WRKY transcription factors in response to temperature stress. *Mol. Genet. Genom.* **2016**, *291*, 255–269. [[CrossRef](#)] [[PubMed](#)]
49. Hellweger, F.L.; Huang, Y.; Luo, H. Carbon limitation drives GC content evolution of a marine bacterium in an individual-based genome-scale model. *ISME J.* **2018**, *12*, 1180–1187. [[CrossRef](#)]
50. Yu, X.; Mo, Z.; Tang, X.; Gao, T.; Mao, Y. Genome-wide analysis of HSP70 gene superfamily in *Pyropia yezoensis* (Bangiales, Rhodophyta): Identification, characterization and expression profiles in response to dehydration stress. *BMC Plant Biol.* **2021**, *21*, 435. [[CrossRef](#)]
51. Gao, T.; Mo, Z.; Tang, L.; Yu, X.; Du, G.; Mao, Y. Heat shock protein 20 gene superfamilies in red algae: Evolutionary and functional diversities. *Front. Plant Sci.* **2022**, *13*, 817852. [[CrossRef](#)]
52. Fujino, A.; Fukushima, K.; Namiki, N.; Kosugi, T.; Takimoto-Kamimura, M. Structural analysis of an MK2-inhibitor complex: Insight into the regulation of the secondary structure of the Gly-rich loop by TEI-I01800. *Acta Crystallogr. Sect. D Biol. Crystallogr.* **2010**, *66 Pt 1*, 80–87. [[CrossRef](#)] [[PubMed](#)]
53. Ishiguro, A.; Kimura, N.; Noma, T.; Shimo-Kon, R.; Ishihama, A.; Kon, T. Molecular dissection of ALS-linked TDP-43—Involvement of the Gly-rich domain in interaction with G-quadruplex mRNA. *FEBS Lett.* **2020**, *594*, 2254–2265. [[CrossRef](#)]
54. Hanano, S.; Sugita, M.; Sugiura, M. Isolation of a novel RNA-binding protein and its association with a large ribonucleoprotein particle present in the nucleoplasm of tobacco cells. *Plant Mol. Biol.* **1996**, *31*, 57–68. [[CrossRef](#)] [[PubMed](#)]
55. Czolpinska, M.; Rurek, M. Plant glycine-rich proteins in stress response: An emerging, still prospective story. *Front. Plant Sci.* **2018**, *9*, 302. [[CrossRef](#)] [[PubMed](#)]
56. Yamaguchi-Shinozaki, K.; Shinozaki, K. Organization of cis-acting regulatory elements in osmotic- and cold-stress-responsive promoters. *Trends Plant Sci.* **2005**, *10*, 88–94. [[CrossRef](#)]
57. Kim, S.Y. The role of ABF family bZIP class transcription factors in stress response. *Physiol. Plant.* **2006**, *126*, 519–527. [[CrossRef](#)]
58. Yamaguchi-Shinozaki, K.; Shinozaki, K. A novel cis-acting element in an *Arabidopsis* gene is involved in responsiveness to drought, low-temperature, or high-salt stress. *Plant Cell* **1994**, *6*, 251–264.
59. Jiang, C.; Iu, B.; Singh, J. Requirement of a CCGAC cis-acting element for cold induction of the BN115 gene from winter Brassica napus. *Plant Mol. Biol.* **1996**, *30*, 679–684. [[CrossRef](#)]
60. Jin, H.; Martin, C. Multifunctionality and diversity within the plant MYB-gene family. *Plant Mol. Biol.* **1999**, *41*, 577–585. [[CrossRef](#)]
61. Zheng, S.; Lin, Y.; Lai, Z.; Lin, J. Isolation and characterisation of a MYB transcription factor associated with epigallocatechin-3-gallate biosynthesis in *Camellia sinensis* L. *J. Horticult. Sci. Biotechnol.* **2019**, *94*, 41–48. [[CrossRef](#)]
62. Yu, Y.; Guo, D.; Li, G.; Yang, Y.; Zhang, G.; Li, S.; Liang, Z. The grapevine R2R3-type MYB transcription factor VdMYB1 positively regulates defense responses by activating the stilbene synthase gene 2 (VdSTS2). *BMC Plant Biol.* **2019**, *19*, 478. [[CrossRef](#)] [[PubMed](#)]
63. Cominelli, E.; Tonelli, C. A new role for plant R2R3-MYB transcription factors in cell cycle regulation. *Cell Res.* **2009**, *19*, 1231–1232. [[CrossRef](#)]
64. Brownfield, L.; Hafidh, S.; Borg, M.; Sidorova, A.; Mori, T.; Twell, D. A plant germline-specific integrator of sperm specification and cell cycle progression. *PLoS Genet.* **2009**, *5*, e1000430. [[CrossRef](#)] [[PubMed](#)]

65. Borg, M.; Brownfield, L.; Khatab, H.; Sidorova, A.; Lingaya, M.; Twell, D. The R2R3 MYB transcription factor *DUO1* activates a male germline-specific regulon essential for sperm cell differentiation in *Arabidopsis*. *Plant Cell* **2011**, *23*, 534–549. [[CrossRef](#)]
66. Hisanaga, T.; Okahashi, K.; Yamaoka, S.; Kajiwara, T.; Nishihama, R.; Shimamura, M.; Yamato, K.T.; Bowman, J.L.; Kohchi, T.; Nakajima, K. A cis-acting bidirectional transcription switch controls sexual dimorphism in the liverwort. *EMBO J.* **2019**, *38*, e100240. [[CrossRef](#)]
67. Hennig, L.; Grisse, W.; Grossniklaus, U.; Köhler, C. Transcriptional programs of early reproductive stages in *Arabidopsis*. *Plant Physiol.* **2004**, *135*, 1765–1775. [[CrossRef](#)]
68. Von Dassow, P.; Ogata, H.; Probert, I.; Wincker, P.; Da Silva, C.; Audic, S.; Claverie, J.-M.; de Vargas, C. Transcriptome analysis of functional differentiation between haploid and diploid cells of *Emiliania huxleyi*, a globally significant photosynthetic calcifying cell. *Genome Biol.* **2009**, *10*, R114. [[CrossRef](#)] [[PubMed](#)]
69. Seo, P.J.; Xiang, F.; Qiao, M.; Park, J.-Y.; Lee, Y.N.; Kim, S.-G.; Lee, Y.-H.; Park, W.J.; Park, C.-M. The MYB96 transcription factor mediates abscisic acid signaling during drought stress response in *Arabidopsis*. *Plant Physiol.* **2009**, *151*, 275–289. [[CrossRef](#)] [[PubMed](#)]
70. Dossa, K.; Mmadi, M.A.; Zhou, R.; Liu, A.; Yang, Y.; Diouf, D.; You, J.; Zhang, X. Ectopic expression of the sesame MYB transcription factor *SiMYB305* promotes root growth and modulates ABA-mediated tolerance to drought and salt stresses in *Arabidopsis*. *AoB Plants* **2019**, *12*, plz081. [[CrossRef](#)]
71. Ambawat, S.; Sharma, P.; Yadav, N.R.; Yadav, R.C. MYB transcription factor genes as regulators for plant responses: An overview. *Physiol. Mol. Biol. Plants* **2013**, *19*, 307–321. [[CrossRef](#)]
72. Yong, Y.; Zhang, Y.; Lyu, Y. A MYB-related transcription factor from *Lilium lancifolium* L. (*LlMYB3*) is involved in anthocyanin biosynthesis pathway and enhances multiple abiotic stress tolerance in *Arabidopsis thaliana*. *Int. J. Mol. Sci.* **2019**, *20*, 3195. [[CrossRef](#)] [[PubMed](#)]
73. Shan, H.; Chen, S.; Jiang, J.; Chen, F.; Chen, Y.; Gu, C.; Li, P.; Song, A.; Zhu, X.; Gao, H. Heterologous expression of the chrysanthemum R2R3-MYB transcription factor *CmMYB2* enhances drought and salinity tolerance, increases hypersensitivity to ABA and delays flowering in *Arabidopsis thaliana*. *Mol. Biotechnol.* **2012**, *51*, 160–173. [[CrossRef](#)] [[PubMed](#)]
74. Park, M.Y.; Kang, J.-Y.; Kim, S.Y. Overexpression of *AtMYB52* confers ABA hypersensitivity and drought tolerance. *Mol. Cells* **2011**, *31*, 447–454. [[CrossRef](#)] [[PubMed](#)]
75. Brawley, S.H.; Blouin, N.A.; Ficko-Blean, E.; Wheeler, G.L.; Lohr, M.; Goodson, H.V.; Jenkins, J.W.; Blaby-Haas, C.E.; Helliwell, K.E.; Chan, C.X.; et al. Insights into the red algae and eukaryotic evolution from the genome of *Porphyra umbilicalis* (Bangioophyceae, Rhodophyta). *Proc. Natl. Acad. Sci. USA* **2017**, *114*, E6361–E6370. [[CrossRef](#)]
76. Collén, J.; Porcel, B.; Carré, W.; Ball, S.G.; Chaparro, C.; Tonon, T.; Barbeyron, T.; Michel, G.; Noel, B.; Valentin, K.; et al. Genome structure and metabolic features in the red seaweed *Chondrus crispus* shed light on evolution of the Archaeplastida. *Proc. Natl. Acad. Sci. USA* **2013**, *110*, 5247–5252. [[CrossRef](#)]
77. Nozaki, H.; Takano, H.; Misumi, O.; Terasawa, K.; Matsuzaki, M.; Maruyama, S.; Nishida, K.; Yagisawa, F.; Yoshida, Y.; Fujiwara, T.; et al. A 100%-complete sequence reveals unusually simple genomic features in the hot-spring red alga *Cyanidioschyzon merolae*. *BMC Biol.* **2007**, *5*, 28. [[CrossRef](#)]
78. Lee, J.; Yang, E.C.; Graf, L.; Yang, J.H.; Qiu, H.; Zelzion, U.; Chan, C.X.; Stephens, T.G.; Weber, A.P.M.; Boo, G.H.; et al. Analysis of the draft genome of the red seaweed *Gracilariopsis chorda* provides insights into genome size evolution in Rhodophyta. *Mol. Biol. Evol.* **2018**, *35*, 1869–1886. [[CrossRef](#)]
79. Lee, J.; Kim, D.; Bhattacharya, D.; Yoon, H.S. Expansion of phycobilisome linker gene families in mesophilic red algae. *Nat. Commun.* **2019**, *10*, 4823. [[CrossRef](#)]
80. Schönknecht, G.; Chen, W.; Ternes, C.; Barbier, G.; Shrestha, R.; Stanke, M.; Bräutigam, A.; Baker, B.; Banfield, J.; Garavito, R.; et al. Gene transfer from bacteria and archaea facilitated evolution of an extremophilic eukaryote. *Science* **2013**, *339*, 1207–1210. [[CrossRef](#)]
81. Price, D.C.; Chan, C.X.; Yoon, H.S.; Yang, E.C.; Qiu, H.; Weber, A.P.; Schwacke, R.; Gross, J.; Blouin, N.A.; Lane, C.; et al. *Cyanophora paradoxa* genome elucidates origin of photosynthesis in algae and plants. *Science* **2012**, *335*, 843–847. [[CrossRef](#)]
82. Gasteiger, E.; Gattiker, A.; Hoogland, C.; Ivanyi, I.; Appel, R.D.; Bairoch, A. ExPASy: The proteomics server for in-depth protein knowledge and analysis. *Nucleic Acids Res.* **2003**, *31*, 3784–3788. [[CrossRef](#)]
83. Bailey, T.L.; Williams, N.; Misleh, C.; Li, W.W. MEME: Discovering and analyzing DNA and protein sequence motifs. *Nucleic Acids Res.* **2006**, *34* (Suppl. S2), W369–W373. [[CrossRef](#)] [[PubMed](#)]
84. Edgar, R.C. MUSCLE: Multiple sequence alignment with high accuracy and high throughput. *Nucleic Acids Res.* **2004**, *32*, 1792–1797. [[CrossRef](#)]
85. Nguyen, L.-T.; Schmidt, H.A.; von Haeseler, A.; Minh, B.Q. IQ-TREE: A fast and effective stochastic algorithm for estimating maximum-likelihood phylogenies. *Mol. Biol. Evol.* **2015**, *32*, 268–274. [[CrossRef](#)] [[PubMed](#)]
86. Wang, Y.; Tang, H.; DeBarry, J.D.; Tan, X.; Li, J.; Wang, X.; Lee, T.-h.; Jin, H.; Marler, B.; Guo, H.; et al. MCS-X: A toolkit for detection and evolutionary analysis of gene synteny and collinearity. *Nucleic Acids Res.* **2012**, *40*, e49. [[CrossRef](#)]
87. Vatansever, R.; Koc, I.; Ozyigit, I.I.; Sen, U.; Uras, M.E.; Anjum, N.A.; Pereira, E.; Filiz, E. Genome-wide identification and expression analysis of sulfate transporter (*SULTR*) genes in potato (*Solanum tuberosum* L.). *Planta* **2016**, *244*, 1167–1183. [[CrossRef](#)] [[PubMed](#)]

88. Zhang, Z.; Li, J.; Zhao, X.-Q.; Wang, J.; Wong, G.K.-S.; Yu, J. KaKs_Calculator: Calculating Ka and Ks through model selection and model averaging. *Genom. Proteom. Bioinform.* **2006**, *4*, 259–263. [[CrossRef](#)] [[PubMed](#)]
89. Lescot, M.; Déhais, P.; Thijs, G.; Marchal, K.; Moreau, Y.; Van de Peer, Y.; Rouzé, P.; Rombauts, S. PlantCARE, a database of plant cis-acting regulatory elements and a portal to tools for in silico analysis of promoter sequences. *Nucleic Acids Res.* **2002**, *30*, 325–327. [[CrossRef](#)] [[PubMed](#)]
90. Tang, L.; Qiu, L.; Liu, C.; Du, G.; Mo, Z.; Tang, X.; Mao, Y. Transcriptomic insights into innate immunity responding to red rot disease in red alga *Pyropia yezoensis*. *Int. J. Mol. Sci.* **2019**, *20*, 5970. [[CrossRef](#)]
91. Brown, J.; Pirrung, M.; McCue, L.A. FQC Dashboard: Integrates FastQC results into a web-based, interactive, and extensible FASTQ quality control tool. *Bioinformatics* **2017**, *33*, 3137–3139. [[CrossRef](#)]
92. Bolger, A.M.; Lohse, M.; Usadel, B. Trimmomatic: A flexible trimmer for Illumina sequence data. *Bioinformatics* **2014**, *30*, 2114–2120. [[CrossRef](#)] [[PubMed](#)]
93. Trapnell, C.; Roberts, A.; Goff, L.; Pertea, G.; Kim, D.; Kelley, D.R.; Pimentel, H.; Salzberg, S.L.; Rinn, J.L.; Pachter, L. Differential gene and transcript expression analysis of RNA-seq experiments with TopHat and Cufflinks. *Nat. Protoc.* **2012**, *7*, 562–578. [[CrossRef](#)] [[PubMed](#)]
94. Chen, C.; Chen, H.; Zhang, Y.; Thomas, H.R.; Frank, M.H.; He, Y.; Xia, R. TBtools: An integrative toolkit developed for interactive analyses of big biological data. *Mol. Plant* **2020**, *13*, 1194–1202. [[CrossRef](#)] [[PubMed](#)]
95. Yu, X.; Wang, L.; Xu, K.; Kong, F.; Wang, D.; Tang, X.; Sun, B.; Mao, Y. Fine mapping to identify the functional genetic locus for red coloration in *Pyropia yezoensis* thallus. *Front. Plant Sci.* **2020**, *11*, 867. [[CrossRef](#)] [[PubMed](#)]
96. Gao, D.; Kong, F.; Sun, P.; Bi, G.; Mao, Y. Transcriptome-wide identification of optimal reference genes for expression analysis of *Pyropia yezoensis* responses to abiotic stress. *BMC Genom.* **2018**, *19*, 251. [[CrossRef](#)]

Disclaimer/Publisher's Note: The statements, opinions and data contained in all publications are solely those of the individual author(s) and contributor(s) and not of MDPI and/or the editor(s). MDPI and/or the editor(s) disclaim responsibility for any injury to people or property resulting from any ideas, methods, instructions or products referred to in the content.